

Computer Techniques in Environmental Studies IV

Editor: P. Zannetti, Failure Analysis Associates, Inc.,
California, USA

Computational Mechanics Publications
Southampton Boston

Co-published with

Elsevier Applied Science
London New York



Uncertainty in Model Calibration Due to Rainfall

T.V. Hromadka II (*), R.J. Whitley (**)

(*) *Boyle Engineering Corporation, Newport Beach, California and California State University, Fullerton, CA 92634, USA*

(**) *University of California, Irvine, CA 92717, USA*

ABSTRACT

In this paper, the unit hydrograph (UH) method is used for the analysis of three model structures for an arbitrary storm event i : (1) a single area UH model noted as $Q_1^i(t)$; (2) an m -subarea link-node model of the catchment, R , with linear unsteady flow routing, and with variable subarea UH's, and where the subarea effective rainfalls are linear in the measured effective rainfall, noted as $Q_m^i(t)$; and (3) an estimator, $\hat{Q}_m^i(t)$, which represents the $Q_m^i(t)$ model except that all model parameters are estimated, and the storm effective rainfall distribution over R is estimated. Available for model calibration purposes is a rain gauge site which is monitored such as to produce an effective rainfall distribution, and a stream gauge located at the downstream point of R .

Using the above three model structures for R , the modeling calibration can be analyzed as to parameter calibration efficiency, reliability, and rationality.

INTRODUCTION

The issue of parameter calibration for hydrologic models has been a topic of considerable concern since the inception of computer modeling techniques. Hromadka and Whitley¹ reviews several of the negative reports obtained from the open literature concerning the lack of success in obtaining "optimum" parameter sets for hydrologic models of all types. Inherent in the cited literature review is the growing weight of evidence that (1) simple models (e.g., a single area unit hydrograph (UH) model) generally can perform as good as or better than complex models (e.g., a highly discretized, link-node model, possibly with a soil-moisture accounting subalgorithm), and (2) the uncertainty in the effective rainfall distribution (rainfall less losses) over the catchment, R , generally is a dominant factor in the uncertainty in hydrologic model output.

In this paper, the unit hydrograph (UH) method is used for the analysis of three model structures for an arbitrary storm event i :

- (1) a single area UH model, noted as $Q_1^i(t)$;
- (2) an m -subarea link-node model of the catchment, R , with linear unsteady flow routing (Hromadka²), and with variable subareas UH's, and where the subarea effective rainfalls are linear with respect to measured effective rainfall monitored at the single available rain gauge site, noted as $Q_m^i(t)$; and
- (3) an estimator, $Q_m^i(t)$, which represents the $Q_m^i(t)$ model except that all model parameters are estimated, and the storm i effective rainfall distribution over R is estimated.

Available for model calibration purposes is a rain gauge site which is monitored such as to produce an effective rainfall distribution, and a stream gauge located at the downstream point of R .

Using the above three model structures for R , the modeling calibration process can be analyzed as to parameter calibration efficiency, reliability, and rationality.

HYDROLOGIC MODEL STRUCTURE

Each of the above three models and modeling assumptions are described in detail in Hromadka², and will not be fully redeveloped herein.

The catchment R is subdivided into m nearly homogeneous subareas, R_j , such that the effective rainfall distribution in R_j is given by $e_j^i(t)$ for storm i where

$$e_j^i(t) = \sum_{k=1}^{n_j^i} \lambda_{jk}^i e_g^i(t - \theta_{jk}^i) \quad (1)$$

where λ_{jk}^i are coefficients, θ_{jk}^i are timing offsets, and $e_g^i(t)$ is the effective rainfall distribution measured at the rain gauge site for storm event i .

The runoff hydrograph from R_j for storm i is $Q_j^i(t)$ where

$$Q_j^i(t) = \int_{s=0}^t e_j^i(t-s) \phi_j^i(s) ds \quad (2)$$

where $\phi_j^i(s)$ is the storm i UH for R_j . Because $\phi_j^i(s)$ is variable between storms, and correlates $Q_j^i(t)$ to $e_j^i(t)$, then whether a UH model or another runoff model is used has no major effect in this analysis. Obviously subarea rainfall-runoff data would be needed to evaluate $e_j^i(t)$ and $Q_j^i(t)$, and hence $\phi_j^i(s)$.

Assuming initially that channel flow routing storage effects are minor, the true runoff hydrograph model for the

response from R from storm i is given by $Q_m^i(t)$ where

$$Q_m^i(t) = \sum_{j=1}^m Q_j^i(t - \tau_j^i)$$

where τ_j^i is the sum of link translation times from stream gauge. The τ_j^i will vary between storms, stream gauges would be required on the links in evaluate the respective travel times for each link, storm, i .

Combining Eqs. (1) and (2) gives the R contribution from storm i ,

$$Q_j^i(t) = \int_{s=0}^t \sum_{k=1}^{n_j^i} \lambda_{jk}^i e_g^i(t - \theta_{jk}^i - s) \phi_j^i(s)$$

where the $\phi_j^i(s)$ is the same UH used in Eq. (2). rainfall-runoff data in R_j would be needed to evaluate several λ_{jk}^i and θ_{jk}^i , as well as the $\phi_j^i(s)$ from Eq

Combining Eqs. (3) and (4) gives the "true hydrograph model for storm i (for translation routing),

$$Q_m^i(t) = \sum_{j=1}^m \int_{s=0}^t \sum_{k=1}^{n_j^i} \lambda_{jk}^i e_g^i(t - \theta_{jk}^i - s) \phi_j^i(s - \tau_j^i)$$

Rewriting the timing of the subarea effective distribution and the subarea UH simplifies Eq. (5) to

$$Q_m^i(t) = \int_{s=0}^t e_g^i(t-s) \sum_{j=1}^m \sum_{k=1}^{n_j^i} \lambda_{jk}^i \phi_j^i(s - \tau_j^i - \theta_{jk}^i)$$

Equation (6) is the output from a m -subarea link-node R , with the effective rainfall distribution properly (by Eq. (1)) in each individual R_j ; and with variable UH's, $\phi_j^i(s)$; and with variable translation flow travel times for each storm, as summed in the τ_j^i .

Given only the effective rainfall distribution at gauge site, $e_g^i(t)$, and the stream gauge measured hydrograph, $Q_m^i(t)$, and assuming the effective distribution on each subarea R_j is given by Eq. (1) assuming that channel link flow routing is given by travel time with a storm-dependent travel time, then for storm event i is assumed that

$$Q_g^i(t) = Q_m^i(t)$$

A single area UH model, $Q_1^i(t)$, correlates $\{e_g^i(t), Q_g^i(t)\}$ by the correlation distribution $\eta^i(s)$ where

$$Q_1^i(t) = \int_{s=0}^t e_g^i(t-s) \eta^i(s) ds \quad (8)$$

Thus for the above assumptions, $Q_m^i(t) = Q_1^i(t)$ where

$$\eta^i(s) = \sum_{j=1}^m \sum_{k=1}^{n_j^i} \lambda_{jk}^i \phi_j^i(s - \tau_j^i - \theta_{jk}^i) \quad (9)$$

Hence the standard single area UH model, $Q_1^i(t)$, and the link node model $Q_m^i(t)$ with subarea rainfall-runoff data and link runoff data sufficient to define all submodel parameters, are equivalent, assuming the subarea effective rainfalls are related to the rain gauge measured $e_g^i(t)$, by Eq. (1).

Equation (6) can be extended to include linear unsteady flow routing (Hromadka²), but the results of Eqs. (7) and (8) would still be valid. Because of the reduction in mathematical notation, only translation flow routing effects will be considered hereafter.

MODEL PARAMETER CALIBRATION

From the above development it is seen that $Q_1^i(t) = Q_m^i(t)$, where $Q_m^i(t)$ is the "true" model.

In practice, an estimator of $Q_m^i(t)$, denoted by $\hat{Q}_m^i(t)$, is used where

$$\hat{Q}_m^i(t) = \sum_{j=1}^m \int_{s=0}^t \hat{e}_j^i(t-s) \hat{\phi}_j^i(s - \hat{\tau}_j^i) ds \quad (10)$$

where hats are notation for estimates. The subarea UH (or kinematic wave (KW) overland flow planes) are empirically defined without rainfall-runoff data. Additionally, the channel flow routing parameters, represented by the $\hat{\tau}_j^i$, are also estimated. It is noted that in Eq. (10), the $\hat{\phi}_j^i$ and $\hat{\tau}_j^i$ may still be variable between storms in order to approximate a specific modeling technique. It is also recalled that detention or backwater effects are assumed to be minor (Hromadka²).

Probably most important in Eq. (10), the R_j effective rainfalls are estimates as only $e_g^i(t)$ data is available. Indeed, the usual practice is to assign the same storm rainfall to each R_j which is measured at the rain gauge, $P_g^i(t)$. Rewrite the estimator, $\hat{Q}_m^i(t)$, in a form comparable to Eq. (6), an recalling Eq. (1),

where the $\hat{\lambda}_j$ are constants, independent of the storm and reflect only the assumed nonhomogeneity in l between subareas. Obviously, the variability in storm magnitude, and also variations in storm time θ_{jk}^i , are all unknown.

Rewriting Eq. (11) again,

$$\hat{Q}_m^i(t) = \int_{s=0}^t e_g^i(t-s) \sum_{j=1}^m \hat{\lambda}_j \hat{\phi}_j^i(s - \hat{\tau}_j^i) ds$$

which is similar in form to the standard single area Writing Eq. (12) in the form of Eq. (8) gives

$$\hat{Q}_m^i(t) = \int_{s=0}^t e_g^i(t-s) \hat{\eta}^i(s) ds$$

where $\hat{\eta}^i(s)$ is the estimated correlation distribution $e_g^i(t)$ and $Q_g^i(t)$.

In comparing the "true" model $Q_m^i(t)$ to the $\hat{Q}_m^i(t)$ of Eqs. (6) and (10), respectively, it is seen differences occur in the correlation distributions and $\hat{\eta}^i(s)$, respectively.

In Hromadka and Yen³, all storms were assumed ca into storm classes $\langle \xi_o \rangle$ such that any two elements in a specific class $\langle \xi_o \rangle$ would result in nearly effective rainfall distributions at the rain gauge such that one would expect nearly identical runoff hydrographs the catchment, R . Consequently in a predictive mode, design storm effective rainfall $e_g^D(t)$ is assumed to the rain gauge site, the storm class $\langle \xi_o \rangle$ is identified that $e_g^D(t)$ is in $\langle \xi_o \rangle$ and the resulting model predicted the random variable

$$[Q_1^D(t)] = \int_{s=0}^t e_g^D(t-s) [\eta_o(s)] ds$$

where $[\eta_o(s)]$ is the distribution of correlation distribution (see Eq. (8)) in correlating rainfall-runoff information storms in class $\langle \xi_o \rangle$. It is recalled that all elements $\langle \xi_o \rangle$ result in nearly an identical effective distribution; consequently, $e_g^D(t)$ being in $\langle \xi_o \rangle$ implies each storm in $\langle \xi_o \rangle$ results in an effective distribution, $e_g^o(t)$, which nearly duplicates $e_g^D(t)$.

Now compare the models $Q_m^i(t)$ and $\hat{Q}_m^i(t)$ for $e_g^o(t) \in \langle \xi_o \rangle$. From Eqs. (8), (9), and (14),

whereas from Eqs. (12) and (13),

$$[\hat{Q}_m^o(t)] = \int_{s=0}^t e_g^o(t-s) [\hat{\eta}_o(s)] ds \quad (15b)$$

But the $\hat{\eta}_o(s)$ must be nearly identical distributions for any element of $\langle \xi_o \rangle$ due to the imprecise (constant) definition of effective rainfalls in each R_j . This "rigidity" in $\hat{\eta}_o(s)$ becomes apparent when studying severe storms of flood control interest, where nonlinear effects approach linearity (Kromadka²). Hence for any element $e_g^o(t)$ in $\langle \xi_o \rangle$, Eq. (15b) is

$$\hat{Q}_m^o(t) = \int_{s=0}^t e_g^o(t-s) \hat{\eta}_o(s) ds \quad (16)$$

That is, the estimator $\hat{Q}_m^o(t)$ would predict nearly identical responses for runoff given nearly identical effective rainfall distributions occurring at the rain gauge site.

But due to the unknown variations in rainfall over R , among other factors, the runoff hydrographs measured at the stream gauge do vary for nearly identical rain gauge measurements. As a result, the unknown variations in effective rainfall are propagated differently between the single area model, $Q_1^o(t)$, and the link-node model estimator $\hat{Q}_m^o(t)$, during the parameter calibration process.

For the $Q_1^o(t)$ model, the correlation of $Q_g^o(t)$ to $e_g^o(t)$ gives a distribution which is a sample from the random variable, $[\eta_o(s)]$.

For the $\hat{Q}_m^o(t)$ model, however, the calibration effort results in a distribution for the model's effective rainfall estimator, now denoted by $\hat{e}_g^o(t)$ for storm class $\langle \xi_o \rangle$.

Hence due to the rigidity in $\hat{\eta}_o(s)$ in neglecting the variations in effective rainfall over R , these variations must be transferred to the parameters used to model $\hat{e}_g^o(t)$ in $\hat{Q}_m^o(t)$. Hence, $[\hat{Q}_m^o(t)]$ essentially becomes for storm class $\langle \xi_o \rangle$,

$$[\hat{Q}_m^o(t)] = \int_{s=0}^t [\hat{e}_g^o(t-s)] \hat{\eta}_o(s) ds \quad (17)$$

where the variations in $[\hat{e}_g^o(t)]$ produce a minor variation in $\hat{\eta}_o(s)$.

THE CALIBRATION PROCESS

In calibrating $Q_1^o(t)$, the data $Q_g^o(t)$ and $e_g^o(t)$ is used to determine $[\eta_o(s)]$.

In calibrating $\hat{Q}_m^o(t)$, the data $Q_g^o(t)$ and the r is used to determine a best fit $\hat{e}_g^o(t)$. But the submodel structure used to compute the effective $\hat{e}_g^o(t)$ typically cannot fit the derived $\hat{e}_g^o(t)$. As a result $\hat{e}_g^o(t)$ becomes a best fit to the integrated effects $\{e_g^o(t), \lambda_{jk}^i, \theta_{jk}^i, n_j^i\}$ as well as errors in the $\{e_g^o(t), \lambda_{jk}^i, \theta_{jk}^i, n_j^i\}$. Consequently, the calibrated $\hat{Q}_m^o(t)$ more error than the $Q_1^o(t)$ model, and cannot account correct uncertainty distribution of output due to the of the $\hat{e}_g^o(t)$ function.

To demonstrate the above discussion, a 25-sub-node model of an idealized catchment is used which the several assumptions leading to $Q_m^i(t)$, (see Fig. single "available" rain gauge is shown as a triangle. Not shown in Fig. 1 are subarea-centered rain gauges downstream stream gauges which are used for $Q_m^i(t)$ "unavailable" to the estimator, $\hat{Q}_m^i(t)$. The catchment is 500 acres in size, with each R_j being 20 acres. A link is a rectangular channel with dimensions of d feet, width = 5 feet, slope = 0.01 ft/ft, and friction factor of 0.015.

Each subarea has its own UH which is assumed function of its time of concentration, T_c , as shown in Fig. 1. Each subarea is assumed to have a uniform loss rate. The stream gauge site is monitored to determine the effective $e_g^o(t)$, (Fig. 1).

To evaluate the calibration process, a series of effective rainfall distributions (i.e., storms $e_g^o(t)$ defined at the rain gauge site, which satisfy that $e_g^o(t)$ is in the same storm class, $\langle \xi_o \rangle$. For $\hat{Q}_m^o(t)$, the effective rainfalls are assumed related to the $e_g^o(t)$ factors λ_j listed in Table 1. Other parameter data listed in this table. The "true" distributions of random variables distributed according to Fig. 3 for timing offsets, θ_{jk}^o , where mean values are listed in Table 1. The "true" runoff hydrographs are developed each storm using $Q_m^i(t)$.

Because $e_g^o(t)$ is fixed, the $\hat{Q}_m^o(t)$ model must have a fixed output. Therefore, because $\hat{\eta}_o(s)$ is fixed, the best fit for $\hat{e}_g^o(t)$ can be developed for each storm class $\langle \xi_o \rangle$. Some of the resulting plots of effective rainfall distributions are shown in Fig. 5.

For $Q_1^o(t)$, the variations in $e_j^o(t)$ are reflected in $\eta_o(s)$ variations. Some of the elements of the set $\{e_j^o(t)\}$ are shown in summation (distribution) graph form in Fig. 6.

From Fig. 5, the set of $\hat{e}_g^o(t)$ plots needed to calibrate the $Q_g^o(t)$ to the single $\hat{\eta}_o(s)$ cannot be duplicated by a loss rate model structure because the storm precipitation is not identical for each event and, therefore, a loss in accuracy must occur during parameter calibration. Additional

TABLE 1. APPLICATION PROBLEM DATA

Subarea R _j	T _c ¹	$\hat{\lambda}_j^2$	$\hat{\lambda}_{jk}^{o3}$	θ_{jk}^{o4}
1	30	1	1	0
2	30	1	1	0
3	45	1	1	0
4	45	1.1	1.1	5
5	30	1.1	1.1	5
6	30	.9	.9	5
7	45	.8	.8	5
8	30	.8	.8	5
9	30	.7	.7	5
10	30	.7	.7	5
11	45	.8	.8	10
12	45	1.	1.	10
13	45	1.	1.	10
14	45	1.3	1.3	10
15	30	1.3	1.3	10
16	30	1.2	1.2	10
17	45	1.2	1.2	10
18	30	1.1	1.1	10
19	30	1.1	1.1	10
20	45	1.	1.	10
21	30	1.	1.	10
22	30	1.	1.	10
23	30	.9	.9	10
24	45	.9	.9	10
25	45	.8	.8	10

Notes:

1. T_c = time of concentration in minutes
2. $\hat{\lambda}_j$ = assumed ratio of effective rainfall at subarea to rain gauge site
3. $\hat{\lambda}_{jk}$ = mean value for λ_{jk}^i . Note that $\bar{\lambda}_{jk} = \hat{\lambda}_j$
4. θ_{jk} = mean value for θ_{jk}^i , in minutes

final calibrated parameters lose some of the physical meaning for what they were intended, in that they reflect variations in effects other than the loss rate.

In Fig. 6, however, the resulting $\eta_o(s)$ plots (summation graph form) are used to populate a frequency distribution for $[\eta_o(s)]$, to develop the uncertainty distribution for $[Q_1^o(t)]$ using $e_g^o(t)$ as the model input.

It is noted that in this application, the estimated $\hat{\lambda}_j$ are assumed "correctly" in that the $\hat{\lambda}_j$ equal the mean value of λ_{jk}^i (see Table 1). Hence in actual applications, the discrepancies between $\hat{e}_g^o(t)$ and $e_g^o(t)$ shown in Fig. 5 could be augmented.

DISCUSSION

The application demonstrates how the unknown effective distribution manifests itself in the single area UH model, and in a discretized link node model, $\hat{Q}_m^i(t)$, storms of a similar class to calibrate model parameter the $Q_1^i(t)$ model, the uncertainties are incorporated UH correlation distribution, $\eta^i(s)$. In the estimator however, the uncertainties are transferred to the rainfall submodel parameters used in $\hat{e}_g^i(t)$.

Because the $\eta^i(s)$ are allowed to freely v frequency distribution $[\eta(s)]$ of the $i(s)$ reflect th modeling uncertainties as well as the important uncer the effective rainfall distribution over R.

With the estimator, $\hat{Q}_m^i(t)$, however, the rainfall estimator, $\hat{e}_g^i(t)$, is usually a fixed model which cannot fit the irregular effective rainfall dist needed to correlate measured runoff data to the $\hat{Q}_m^i(t)$ correlation distribution, $\hat{\eta}^i(s)$. As a result, the ca of $\hat{e}_g^i(t)$ must be imprecise and, therefore, the $\hat{Q}_m^i(t)$ a more uncertain model in the predictive mode than th model.

CONCLUSIONS

The unit hydrograph method is used to evaluate how uncertainty is propogated through a single area UH mod discretized link node model estimator. It is shown modeling uncertainties and the important uncertainty effective rainfall distribution over the catchm manifested in the single area model unit hydrograph, they are manifested in the link node model est effective loss rate function. Because the effective l submodel is of a prescribed structure, the calibration loss rate submodel of the link node model will re imperfect fits of the effective rainfall distribution to correlate the measured runoff data to the hydraulic function.

In comparison, calibration of the single area (results in the several uncertainties (including b response uncertainties and the unknown distribut effective rainfall over the catchment) being integrat the UH, with the loss rate submodel being calibrated rate information.

REFERENCES

1. Hromadka II, T.V. and Whitley, R.J. (1988), The Storm Concept in Flood Control Design and P Stochastic Hydrology and Hydraulics, in-press.

2. Hromadka II, T.V. (1988), Back to the Unit Hydrograph Method, Proceedings: Envirosoft 88 Conference, Computational Mechanics, Porto Carras, Greece.
3. Hromadka II, T.V. and Yen, C.C. (1988), Unit Hydrograph Models and Uncertainty Distributions, Proceedings: Environsoft 88 Conference, Computational Mechanics, Porto Carras, Greece.

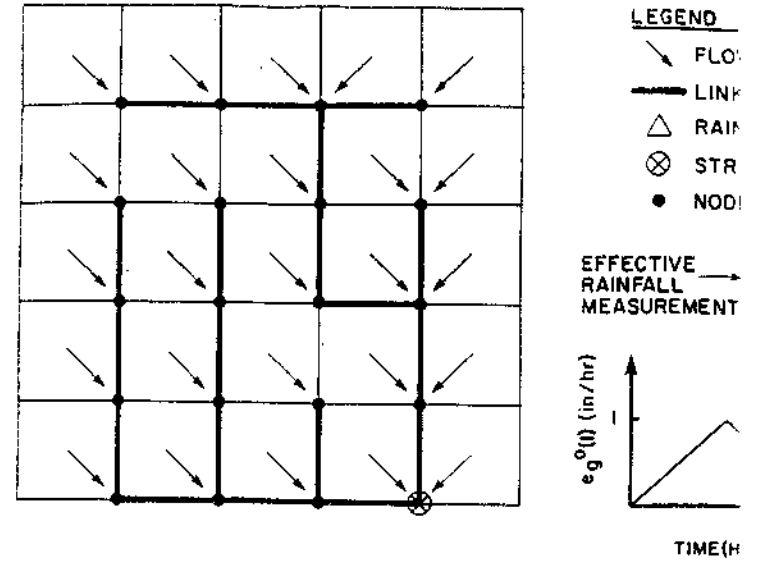


Figure 1. Application Problem Schematic.

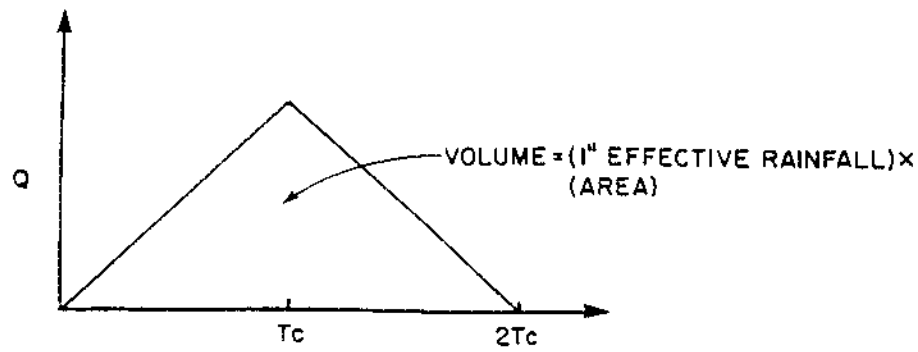


Figure 2. Subarea Unit Hydrograph.

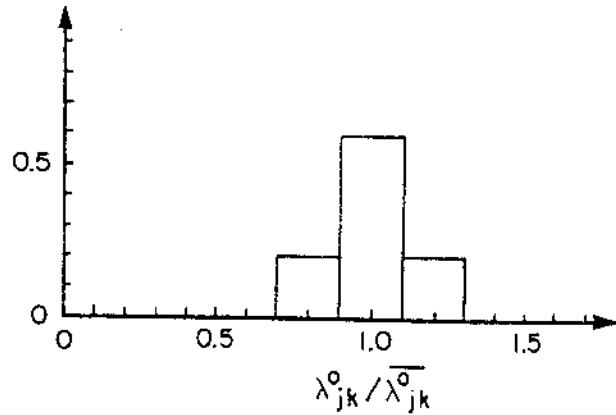


Figure 3. Frequency Distribution for $\lambda^0_{jk}/\lambda^0_{jk}$ (see table 1 for subarea λ^0_{jk}).

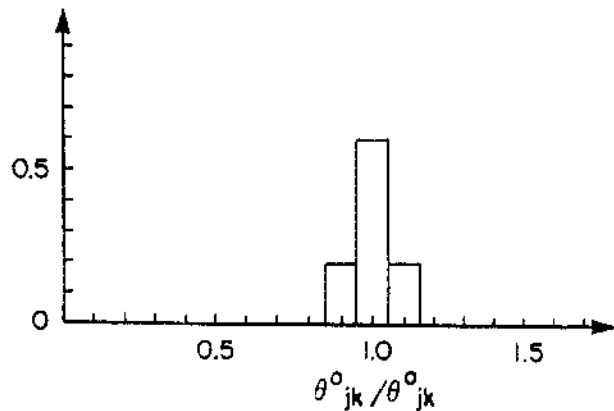


Figure 4. Frequency Distribution for θ^0_{jk} (see table 1 for subarea θ^0_{jk}).

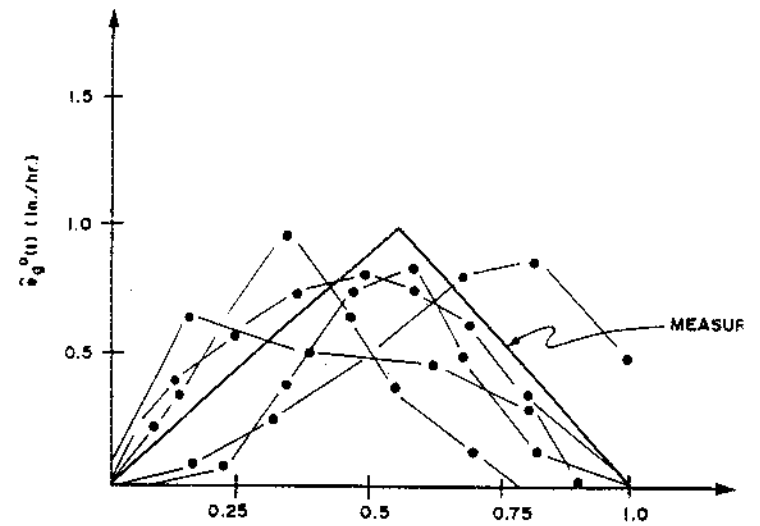


Figure 5. Some Least-Squares Best Fit Effective Rainfall Distributions, $\hat{e}_g^0(t)$ which Correlate Measured Runoff, $Q_g^0(t)$, to the $\hat{\eta}_0(s)$ us Estimator, $\hat{Q}_m^0(t)$, for the Application

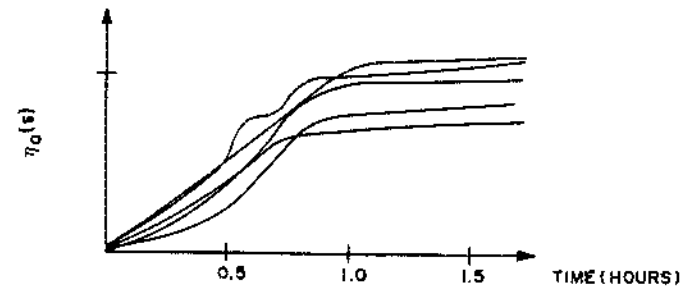


Figure 6. Some Correlation Distributions $\eta^0(s)$ Correlating $Q_g^0(t)$ and $e_g^0(t)$ for the Application Problem, Plotted in Summary (Distribution) Graph Form.